Studies on properties of temperature-sensitive amphiphilic copolymer-modified PVDF ultrafiltration membrane

Feifei Shen, Tonghu Xiao*, Lina Han, Shanmei Chen

Faculty of Materials Science and Chemical Engineering, Ningbo University, Ningbo, 315211 Zhejiang, China
Tel. +86 0574 87600394; Fax: +86 0574 87605484; email: xiaotonghu@nbu.edu.cn

ABSTRACT

A series of temperature-sensitive poly-N-isopropyl acrylamide-*co*-polyethylene glycol methyl methacrylates (NPGs) containing different mass ratios of N-isopropyl acrylamide and poly(ethylene glycol) methacrylate (PEGMA) were synthesized successfully. Each of the NPGs were blended with poly(vinylidene fluoride) to prepare ultrafiltration membranes which have temperature sensitivity and higher hydrophilicity. Both the properties were found to be dependent on the synthesis reaction conditions of NPGs. The morphologies of the membranes were characterized by scanning electron microscopy. With PEGMA content increasing in NPGs, the structures of pure membrane and blended membranes changed from typical asymmetric morphology with short finger-like pores to macrovoid. With the temperature or PEGMA content increasing, the water fluxes of both increased obviously. For example, when the PEGMA content was the highest, the water flux of the blended membrane increased up to 3.2 times compared with pure membrane at 55°C. Bovine serum albumin (67 kDa), polyethylene glycol (50 kDa), polyethylene glycol (20 kDa), and rejection measurements of the blended membrane (e.g. M_3) were conducted in this work. The rejection of the same membrane to different molecular weight substances changed greatly with temperature changing from 10°C to 60°C, which made it possible to separate substances by controlling temperature.

Keywords: Temperature-sensitive membrane; Poly(vinylidene fluoride); Blend modified; Ultrafiltration

1. Introduction

In recent years, ultrafiltration membranes have been paid more and more attention because they can effectively remove bacteria, viruses, and organic macromolecules, and have a series of advantages, such as high separation efficiency, high degree of automation, low energy consumption, and no secondary pollution [1]. However, most commercial ultrafiltration membranes are made from hydrophobic polymers, such as polyethersulfone (PES), polysulfone (PS), polypropylene (PP), and PVDF [2]. PVDF has received great attention as a membrane material due to its outstanding properties, such as high mechanical strength, thermal stability, chemical resistance, and high hydrophobicity compared with other commercialized polymeric materials. So far, PVDF has gained popularity in industries and academia as a suitable membrane material for membrane distillation

*Corresponding author.

[3] and pervaporation [4,5]. PVDF membranes have been extensively applied in ultrafiltration for general separation purposes [6–9]. But, the PVDF is a very hydrophobic material with low surface energy, resulting in low water flux after contamination deposition, and so the biggest limitation of membranes is the continuous declination of flow through the membrane due to fouling [10]. Therefore, to improving the hydrophilic properties of the PVDF is particularly important. Furthermore, due to the membrane pore size constraints, it can only separate substances of a specific molecular weight. The separation of two or more different molecular weight substances often requires the aperture of several different filtration membranes with multiple filters, which makes the separation process more complicated and the cost higher [11]. However, stimuli-responsive membranes that can change their permeation or separation properties have been the focus of research for the last few decades [12–14]. The membrane pore size and distribution can rely on environmental change, so as to achieve the separation of different molecular weight substances. Temperature is the most widely used stimulus in environmental responsive polymer systems. The change of temperature is not only relatively easy to control, but also easily applicable [15]. The common characteristic of temperature-sensitive polymers is the presence of hydrophobic groups, such as methyl, ethyl, and propyl groups. Of the many temperature-sensitive monomers containing hydrophobic groups, N-isopropyl acrylamide (NIP-AAm) is probably the most extensively used monomer [16]. Copolymerization of NIPAAm with different types of monomers results in copolymers with temperature-sensitive property. In water, the copolymer containing the monomer NIPAAm is hydrophilic and exists in a random coil below the lower critical solution temperature (LCST). Above the LCST, however, the copolymer becomes hydrophobic and changes its conformation from a random coil to a globule, and then aggregates due to the hydrophobic interaction among the isopropyl groups [17–19].

The reported temperature-sensitive membranes are generally microfiltration gating membranes through grafting method [20–22]. Especially, the positive and negative gating membranes attracted more attention of scientific researchers. Investigations were systematically carried out on the relationships between the grafting yield with the water flux, the responsiveness coefficient, and the temperature-responsive gating factor of pore size [23,24]. Li [23] reported that when the grafting yield was smaller than 2.81%, both the flux responsiveness coefficient and the thermoresponsivity of the membrane pore size increased with an increase in the grafting yield; however, when the grafting yield was higher than 6.38%, both the flux responsiveness coefficient and the thermoresponsivity of the membrane pore size were always equal to 1; i.e. no gating characteristics existed anymore. In recent years, there have been several reports concerning temperature-sensitive grafted ultrafiltration membranes in the literatures [25–28]. The changes of water fluxes of the grafted membranes with temperatures have become the focus of the studies. But there are few reports concerning the different rejections of the temperature-sensitive ultrafiltration membranes to different molecular substances. However, on one hand, it is difficult to control the graft conditions and to achieve industrialization, and on the other hand, the distribution of the graft polymer is not uniform. In contrast, the distribution of polymers blended in the membrane is uniform and the ratio of polymer/membrane material is adjustable [29,30]. In this research, a series of amphiphilic temperature-sensitive copolymers have been synthesized and blended with PVDF to prepare ultrafiltration membranes. The temperature sensitivity and rejection to different molecular substances of these membranes were systematically investigated.

2. Experimental

2.1. Materials

NIPAAm, (Aldrich); poly(ethylene glycol) methacrylate (PEGMA, Aldrich); tert-butanol; Isopropyl alcohol (IPA); 2,2′-Azobis(2-methyl propionitrile) (AIBN); poly(vinylidene fluoride) (PVDF); N,N-dimethylacetamide (DMAC); Bovine serum albumin (BSA, $M_w = 67$ kDa); Polyethylene glycol (PEG, $M_w = 50$ kDa, $M_w = 20$ kDa); Bismuth(III) Subnitrate; Potassium iodide; and Sodium acetate. BSA was purchased from Aoboxing Biotechnology Limited Company. All other reagents were analytic grades.

2.2. Polymerization

Copolymerization of NIPAAm with PEGMA was carried out in tert-butanol. 2,2′-Azobis (2-methylpropionitrile) (AIBN) (3% relative to monomers) was an initiator. This solution was stirred at 20°C under a nitrogen atmosphere for 30 min in order to remove the oxygen thoroughly. After that, polymerization was conducted at 88°C for 6 h. Then, the unreacted monomer precipitated was removed with n-hexane. Next, the solvent was removed by distillation under reduced pressure, and a pale yellow copolymer was obtained. The above reaction scheme was as follows (see Fig. 1).

Copolymer has been designed as an NPG followed by numerical suffix indicating the mass ratio of the monomers in the initial feed. For example, copolymers prepared by taking 0.6:1, 1.2:1, 1.8:1, and 2.4:1 of NIPAAm/PEGMA were designed as NPG-0.6, NPG-1.2, NPG-1.8, and NPG-2.4, respectively.

To compare the temperature-sensitive performance of NPG, a series of NPGs were prepared by changing the mass ratios of the two monomers as shown in Table 1.

2.3. NPG Characterization

The number average molecular weight (M_n) and polydispersity index (M_w/M_n) of NPGs were determined by gel permeation chromatography (GPC, Waters 1515 Solvent Delivery System, Tokyo, Japan). The chloroform was used as the eluent at a flow rate of 1.0 mL/min and polystyrene as the calibration standard. The number average (M_n) and weight average (M_w) molecular weight of the obtained copolymer (NPG-1.8) were 31.937 K and 78.712 K, with a polydispersity index of 2.464, respectively. While, the M_n of the other obtained copolymers (NPG-0.6, NPG-1.2, and NPG-2.4) were 28.164 K, 31.057 K, and 39.483 K, the M_w were 64.848 K, 65.713 K, and 81.360 K,

Table 1
Details of feed composition for copolymers prepared using IPA [3%(w/w)] as initiator and tert-butanol as solvent

Copolymer	NIPAAm	PEGMA
NPG-0.6	0.6	1
NPG-1.2	1.2	1
NPG-1.8	1.8	1
NPG-2.4	2.4	1

with polydispersity index values of 2.333, 2.088, and 2.061, respectively.

The PEGMA content in the NPGs was calculated by ^{1}H NMR, which was carried out in an AVANCE III spectrometer operating at 400 MHz. Solvent for nuclear magnetic resonance (NMR) spectroscopy was tetrahydrofuran and the internal standard was tetramethylsilane.

FTIR measurement was performed on a Thermo Fisher IR200 infrared spectrometer with KBr pellets.

The LCSTs of the NPGs solutions were measured with UV–vis spectrophotometer by monitoring the turbidity of the NPGs solutions as a function of temperature at 500 nm reported in the literature [31]. The LCST values were determined at 50% transmittance [32]. The LCSTs of the NPGs solutions were at a

Fig. 1. The synthesis route of the P (NIPAAm-*co*-PEGMA) copolymer.

temperature at 50% light transmittance. 1 g of the NPGs was added to a proper amount of deionized water to obtain 2 wt.% solutions.

2.4. Membrane preparation

Membranes were prepared by casting solution method. For this, PVDF, IPA, and NPG copolymers were dissolved in DMAC with stirring at 78℃ and the solutions were allowed to stand overnight to release the bubbles. The solution was cast on a clean glass plate, and then it was immersed immediately into a bath of water at constant temperature of 25℃. The obtained membrane was removed from the bath after complete separation and saved in deionized water. The composition of the casting solution is listed in Table 2.

2.5. Membrane characterization

2.5.1. SEM

Morphologies of prepared membranes were observed by SEM (S-4700, Hitachi Limited, Japan).

2.5.2. DSC

The thermal and crystal behaviors of membranes were determined using Differential Scanning Calorimeter (DSC) (PyrisDiamond, Perkin–Elmer, US). Each sample was heated from 25.00℃ to 180.00℃ at 10.00℃/min, held for 1 min at 180.00℃, and then cooled from 180.00℃ to 25.00℃ at 10.00℃/min in a nitrogen atmosphere.

2.5.3. Membrane hydrophilicity

Water contact angles (CA) were measured with an anglemeter (OCA-20 contact angle system, Beijing

Table 2
Details of composition and sample designation for membranes prepared using casting solution method

Code	PVDF (%)	NPG (%)	DMAC (%)	IPA (%)
M_0	10	0	87	3
M_1(NPG-0.6)	9	1	87	3
M_2(NPG-1.2)	9	1	87	3
M_3(NPG-1.8)	9	1	87	3
M_4(NPG-2.4)	9	1	87	3

The numerals within parentheses represent the samples prepared using various NPG copolymers. The letter (NPG-0.6, i.e.) within parentheses represents the copolymers blended in the membranes.
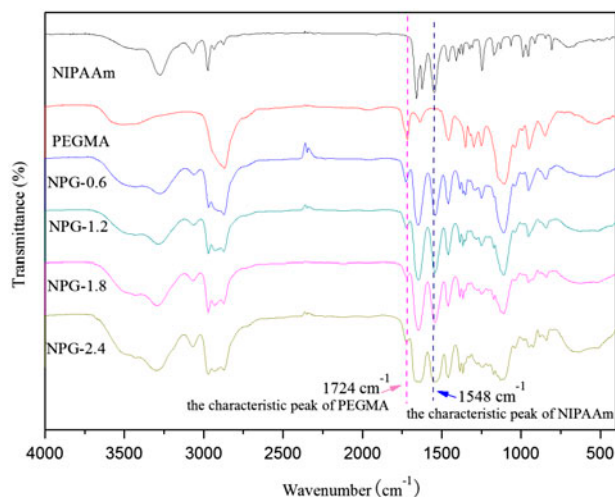
Jinshengxin Instruments, Inc., China) at 25℃. The deionized water was dropped on the sample surface at five different sites. Each of the measured values from three independent membranes were taken as their water contact angles.

2.5.4. Water flux and rejection

The ultrafilter cup (MSC300) with temperature control equipment was used to measure the membranes' performance under a pressure of 0.1 MPa. The effective membrane area was $35 \, cm^2$. The pure water flux was measured three times, and the water temperature was changed from 10℃ to 60℃. Pure water flux (J_{wi}) was calculated by the following equation (Eq. 1).

$$J_{wi} = V/At \tag{1}$$

where V is the volume of permeated water (L), A is the effective membrane area (m^2), and t is the ultrafiltration time (h).

BSA rejection measurement was conducted at 0.1 MPa with 1.0 g/L BSA solution. The concentrations of protein in the feed and permeate solutions were measured immediately after collection using an UV–vis spectrophotometer (UV-7504C, China) at 280 nm. The rejection of membrane, R, can be defined as follows:

$$R \, (\%) = (1 - C_p/C_f) \times 100 \tag{2}$$

where C_p represents permeate concentration and C_f represents feed concentration.

The PEG 50 kDa and PEG 20 kDa rejection measurements were tested at 510 nm with Dragendoff reagent as chromogenic agent.

3. Results and discussion

3.1. NPGs characterization

3.1.1. FTIR analysis

Fig. 2 shows the FTIR spectra of the monomers NIPAAm and PEGMA, and the copolymer NPGs, respectively.

In comparison with the monomers and NPGs, the absorption bands associated with the PEGMA at $1,724 \, cm^{-1}$ (symmetrical C=O stretching), $1,636 \, cm^{-1}$ (C=C stretching), and $1,106 \, cm^{-1}$ (C–O stretching) were presented in all of the NPGs samples, which is similar to the data reported [33,34]. Compared with

Fig. 2. FTIR spectra of NIPAAm, PEGMA, and NPGs.

the FTIR spectra of the monomers, the absorption bands of NPGs at 1,645 and 1,548 cm^{-1} can be attributed, respectively, to the secondary amide C=O stretching and N–H stretching of the amide (O=C–NH) groups of the NIPAAm chain [35].

3.1.2. ^{1}H NMR of copolymer (e.g. NPG-1.8)

^{1}H NMR spectra were taken with a Bruker Avance 400 (400 MHz) spectrometer in CDCl$_3$. A typical ^{1}H NMR spectrum of the NPG-1.8 is shown in Fig. 3.

The results were as follows: ^{1}H NMR (CDCl$_3$, δ ppm): 1.0–1.4 (d, 6H,–CH–(CH$_3$)$_2$), 1.5 (m, 3H, CH$_3$–C–C = O–), 3.5–3.7 (m, 4H, –O–CH$_2$CH$_2$–), and 3.9–4.1 (m, 1H, –CH–(CH$_3$)$_2$) [36]. The NPG-1.8 composition was estimated by comparing the peak area of methane protons (*e*) from NIPAAm with methylene protons (*d*) from PEGMA in the same figure. The mass feed ratio NIPAAm/PEGMA of the NPG-1.8 was determined by comparing the intensity of the characteristic peak signals *e* and *d*. Thus, the NIPAAm/PEGMA mass ratio could be calculated as 1.84:1, which was consistent with the target product designed.

3.1.3. Effect of monomer concentration on LCST

The cloud points of the NPGs in water were estimated by means of transmittance measurements of NPGs' aqueous solutions. Fig. 4 shows transmittance vs. temperature curves for all the NPGs with different contents of monomers and the transmissions decreased above the LCST obviously. It was because of chain collapse and aggregation in solution, as has been established for NPGs [37]. These data show that all the NPGs

had very sensitive and different transmittance changes in a distinctly narrow temperature range. The LCST of NPG-0.6, NPG-1.2, NPG-1.8, and NPG-2.4 were 43.9℃, 54.0℃, 46.8℃, and 45.4℃, respectively. With decreasing content of PEGMA, the LCST of the copolymer solutions first shifted to a higher temperature and then turned to a lower one. The LCST of NPGs is attributed to a change in the hydrophilic/hydrophobic balance of the polymers with respect to the hydrophobic and H-bond interactions of water molecules with the polymer chain. At low temperature, strong H-bonding interactions between polar groups and water lead to good solubility of the polymer, which is opposed by the hydration of apolar groups. The water surrounding the apolar groups is in a low entropy state relative to free water, leading to an entropic penalty. As the apolar surface area of the polymer increases, this entropic penalty increases and the LCST decreases [26]. In this work, the addition of PEGMA in NPGs made the polar of NPGs increase, so that the LCST of NPGs increased. All the copolymers exhibited higher LCSTs (43.0–54.0℃) than poly(N-isopropyl acrylamide) (nearly 32℃) [38,39] in the water solution. It indicates that the LCST of NPGs could be controlled only by changing the feed ratio of the monomers at copolymerization.

Fig. 5 shows the schematic of the behavior of NPGs during heating and cooling, which explains what has happened during the shrinking of the chain backbone in Fig. 4. At lower temperature, each copolymer chain in water exists as a random coil. The heating makes the PNIPAAm chain backbone insoluble in water so that it undergoes the coil-to-globule transition, which has been reported in the literature [40]. In this process, the hydrophilic PEGMA chains are forced to stay on the periphery of the globule to form a core-shell nanostructure, such as the one schematically shown in Fig. 5. Thus, the polymer solution had a higher light transmittance rate. As the temperature increased, the hydrophobic property of the NPGs enhanced. When the temperature was higher than the LCST, the solvate shell of NPGs was destroyed and the water molecules were discharged from the solvation shell. As a result, phase transition occurred and the copolymer solution became turbid. When the temperature was lower than the LCST, the solution became clear again. In conclusion, the phase transition was reversible.

3.2. Membrane characterization

3.2.1. Compatibility of the blended membrane

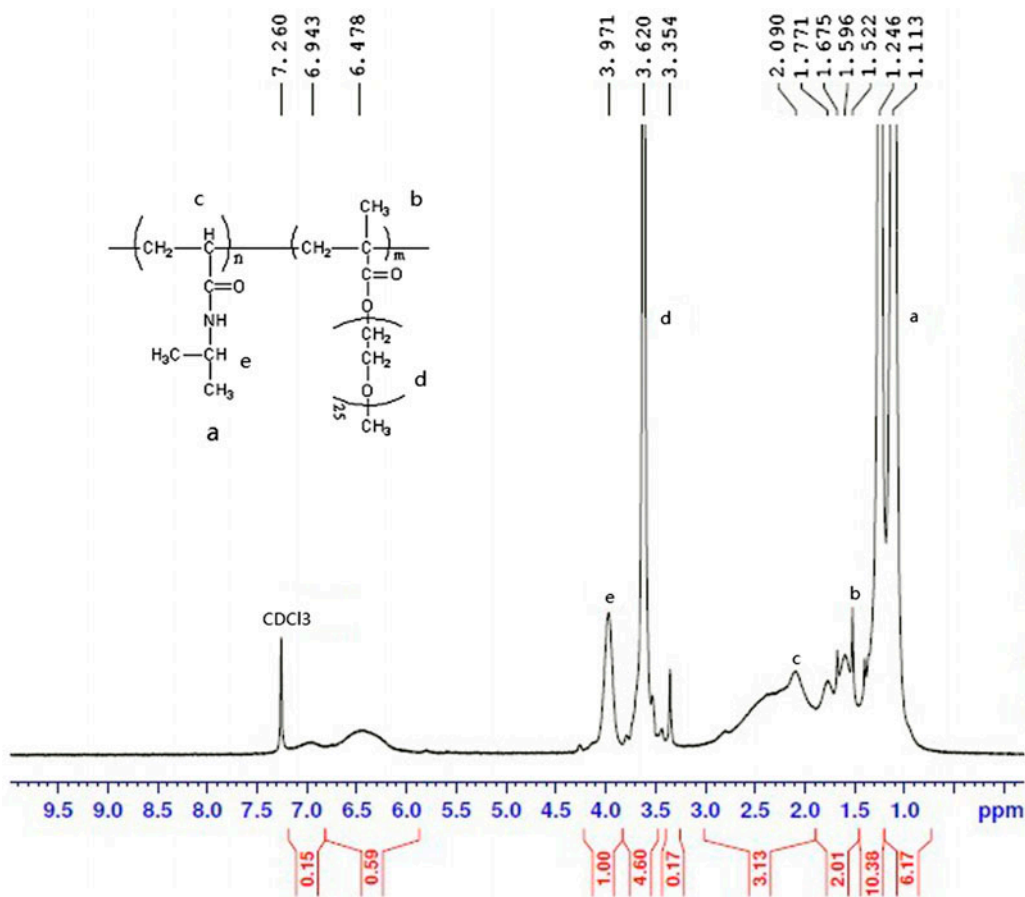The compatibility of the two different component polymers in the blended membrane is examined from

Fig. 3. ^{1}H NMR spectrum obtained for NPG-1.8 in CDCl$_3$.

their thermal behaviors. The thermal and crystal behaviors of blended membranes were determined
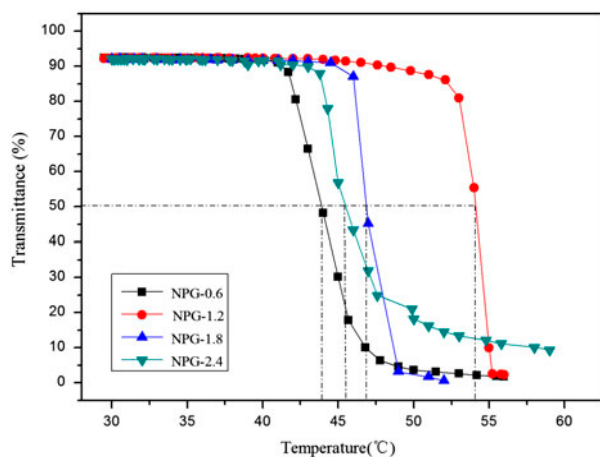

Fig. 4. Transmittance vs. temperature curves for 2.0 wt.% NPGs aqueous solutions.

using differential scanning calorimeter (DSC). If single crystallization is observed for the blended membranes, it indicates good compatibility of the blended membranes, which has been reported in the literature [41,42].

The DSC traces of the blended membranes are given in Fig. 6. An exothermic peak corresponding to the freezing of crystalline phase of NPG-1.8 was observed at 103.0℃ (see Fig. 6(a)). The pure PVDF membrane has the highest crystallization temperature. The crystallization temperature of blended membranes shifted to lower values on incorporation of different NPGs as shown in Fig. 6(b). The pure PVDF membrane (M_0) was at 153.7℃, while the blended membranes (M_1, M_2, M_3, and M_4) were at 153.1℃, 152.6℃, 151.9℃, and 151.3℃, respectively. Single crystallization is observed for the blended membranes containing NPGs, indicating good compatibility of the blended membrane. It can also be seen from Fig. 6(c) that the crystallization temperature of the membranes decreased with increase in NPGs' concentration in the
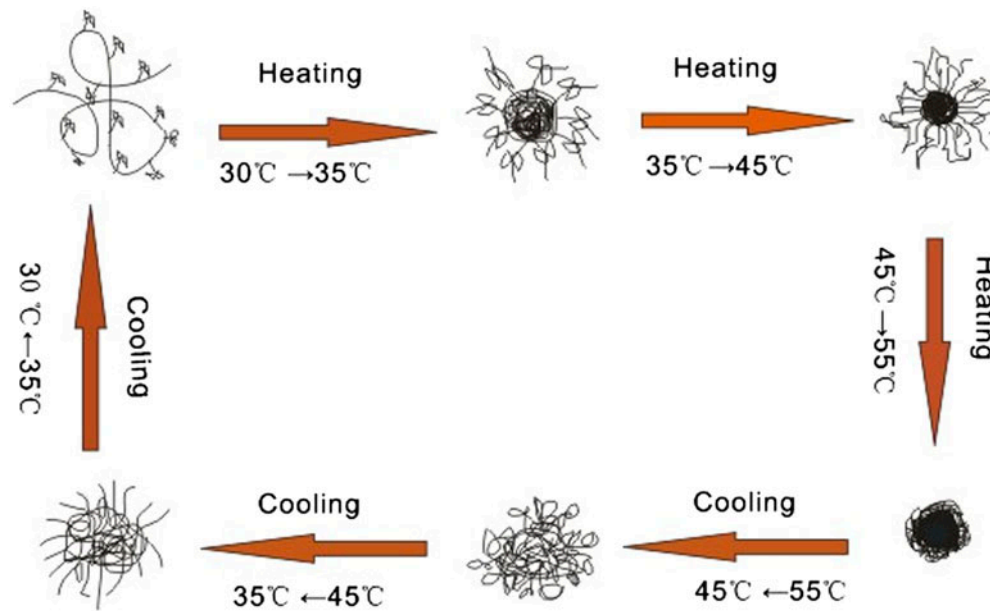
Fig. 5. The schematic of the behavior of NPGs during heating and cooling.

blended membranes, though the effect is small. This is because the crystallization temperature of NPGs is lower after blending it with PVDF, and it is fully compatible with PVDF. Therefore, with the increase of its content, the crystallization temperature of the membrane decreases.

3.2.2. Morphologies of the pure and modified PVDF membranes

The morphologies of the pure membrane (M_0) and modified membranes (M_1–M_4) were studied by SEM. In Fig. 7, the cross-section of the membranes was monitored at a magnification of 1,000×. After blending by NPGs, the morphologies of the modified membranes revealed an obvious change when Fig. 7(a) (M_0) is compared with Fig. 7(b)–(e). The cross-section of M_0 showed typical asymmetric morphology with short finger-like pores linked by sponge structures. All the blended membranes exhibited macrovoid formation in the cross-sections.

As many literature studies have shown, the presence of amphiphilic polymers will have an impact on the process of phase separation and membrane final morphology and structure. As reported by Kesting [43], the presence of an amphiphilic polymer in the casting solution can enhance the solvent–non-solvent exchange by increasing the affinity of the casting solution and water, therefore creating favorable condi-

tions for instantaneous liquid–liquid demixing and forming short finger-like structures. Fig. 7 shows that the temperature-sensitive polymers NPGs as amphiphilic polymers affected on the membrane structure when blended with PVDF, which is consistent with the literature [44]. When the content of the monomer in NPGs was increased, the membrane material had a better affinity with non-solvent water, and the speed of the phase separation was faster, and thus the macrovoids formed easily [44,45].

3.2.3. Membrane hydrophilicity

Hydrophilic polymers were blended with the hydrophobic PVDF membrane materials, leading to increased hydrophilicity of the blended membranes. The water contact angle is an important parameter in measuring the surface hydrophilicity and wetting properties. In general, the lower the contact angle, the higher the hydrophilicity of the membrane surface. As for as the blended method for membrane surface modification, the polymerization conditions' dependence on the water contact angle was plotted to study the effect of the monomer concentration on surface hydrophilicity. The variation of the water dynamic contact angle membranes blended with the NPGs with different monomer ratios is shown in Fig. 8. The contact angle of the pure PVDF membrane was about 84°, which is comparable to the value obtained by
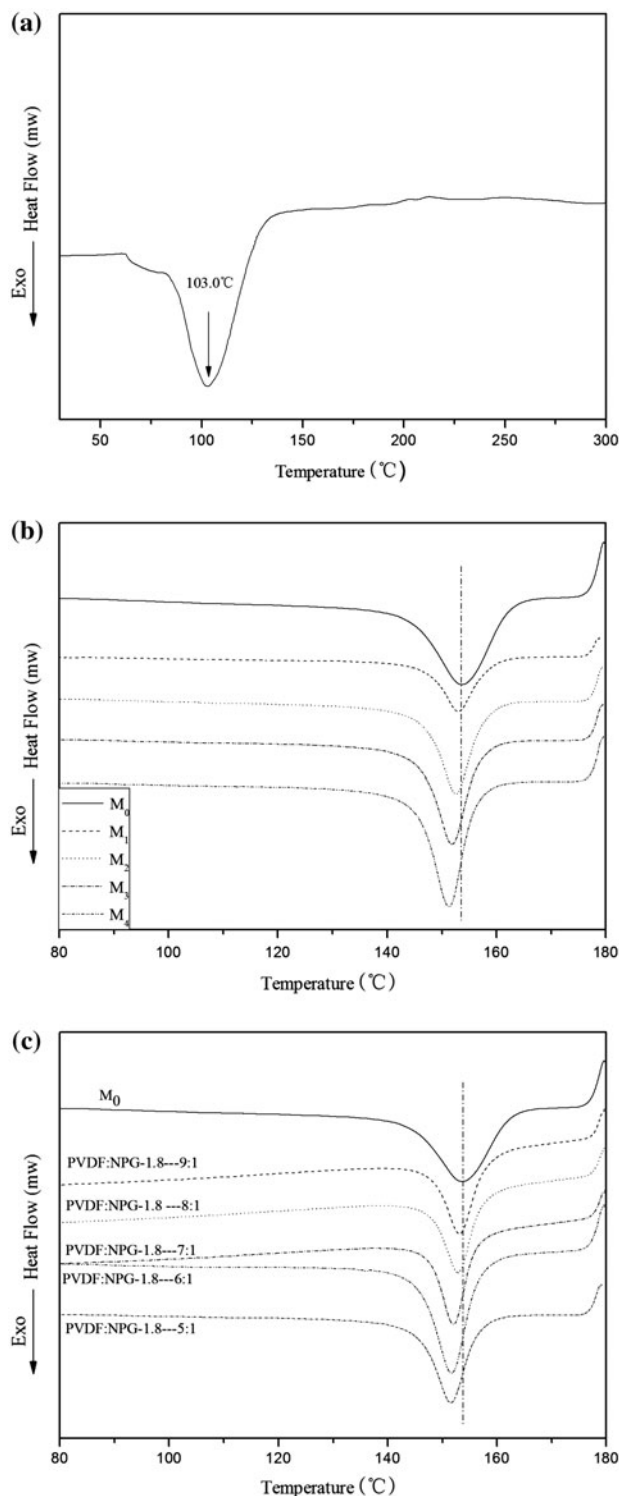
Fig. 6. DSC curves of NPG-1.8 (a) membranes M_0–M_4 and (b) membranes with different proportions of NPG-1.8 (c).

Chang for a similar membrane [46]. It can be seen that the contact angle decreased with the increased content of PEGMA in NPGs: the contact angle

dropped to 63° after 180 s for the highest content of PEGMA. The contact angle decreased to 70° for NPG-2.4, 69° for NPG-1.8, and 66° for NPG-1.2 after 180 s. This reason might be due to the increasing amount of ethyl oxide side groups in the PEGMA polymer chain in the membrane [47]. The decrease of contact angle was obvious, which is especially true for the monomer PEGMA, indicating a switch from a hydrophobic surface to a hydrophilic surface blended with NPGs.

3.2.4. Temperature-dependent pure water flux through the blended UF membranes

The effect of temperature on the water flux of the blended membranes is shown in Fig. 9. The water flux of pure membrane increased slightly with rising temperature, while the blended membranes increased obviously. Meanwhile, M_1 had the highest value and M_4 had the lowest. It is clear that the water fluxes of the blended membranes depend little on the temperature when the temperature is lower than 40℃. However, when the temperature rose higher than 45℃, the flux of the water increased significantly near the LCST of the NPGs. Take M_1 for example; the flux of water at 55℃ is almost four times higher than that at 25℃. The change of NPGs on the surface of the membranes at different temperatures is schematically depicted in Fig. 10. At lower temperature, each copolymer chain in water exists as a random coil. When the temperature was higher than LCST, it underwent the coil-to-globule change which caused an increase in pore sizes, and which further increased the water flux of membranes.

In addition, it can be seen from Fig. 9 that all the blended membranes exhibited higher water fluxes than the pure PVDF membrane at the same temperature. At last, the water fluxes of membranes M_0–M_4 also increased with the content of PEGMA in NPGs. Especially after 35 ℃, the water fluxes increased significantly with PEGMA monomer increase in NPGs. For example, the water fluxes of M_1–M_4 were 1006.0 L m^{-2} h^{-1}, 661.2 L m^{-2} h^{-1}, 622.1 L m^{-2} h^{-1}, and 544.4 L m^{-2} h^{-1} at 55℃, while M_0 was 315.8 L m^{-2} h^{-1}. The values of water fluxes increased 3.2 times, 2.1 times, 1.9 times, and 1.7 times compared with M_0. The increase of water fluxes is probably due to the macrovoids of M_1 and M_2 which to the decrease of resistance of their support layer and the increase of the water flux. This result is in confirmation with the morphologies of the pure and modified PVDF membranes as shown in Fig. 7. Meanwhile, the hydrophilicity of membranes have some influence to a
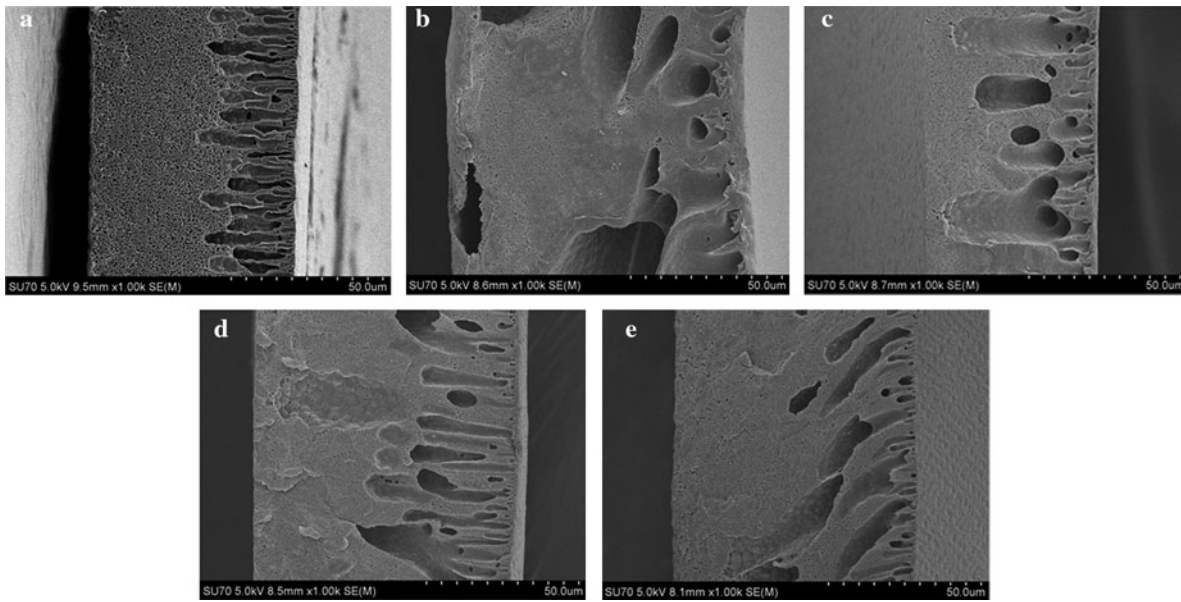
Fig. 7. SEM images of the cross-section membranes M_0–M_4; (a) M_0, (b) M_1, (c) M_2, (d) M_3, and (e). M_4 (the right side was the top skin layer of membranes).
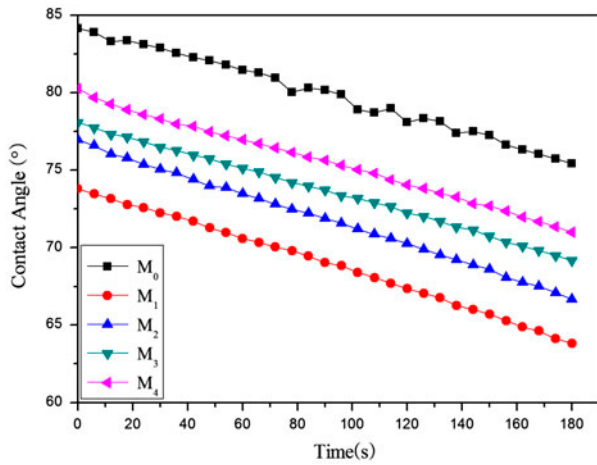

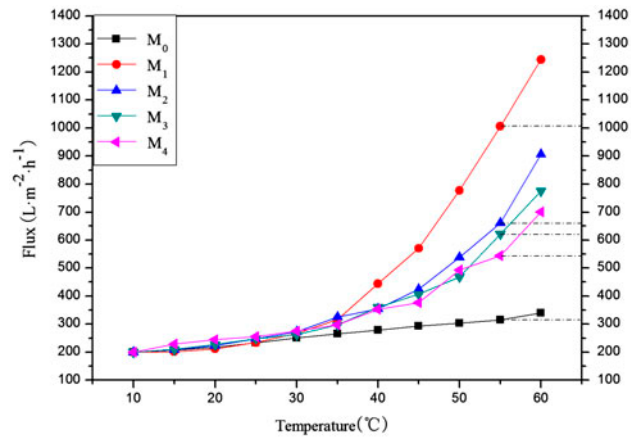Fig. 8. Effect of PEGMA content in NPGs on the water contact angle.

Fig. 9. The relationship between the fluxes of pure water and temperature for the membranes M_0–M_4.

certain extent as shown in Fig. 8. It shows that the blended membranes had a good performance of temperature sensitivity.

The membranes M_1 and M_2 showed higher temperature-dependent pure water fluxes compared to the membranes M_3 and M_4, but their mechanical strengths were poor. So, the membranes M_3 and M_4 were selected for further study.

3.2.5. Comparison of rejection of the temperature-sensitive membranes (M_3, M_4) with different substances

The relationship between the different molecular weight substances and the rejection property of M_3 was investigated with 1.0 g/L BSA, PEG (50 kDa) and PEG (20 kDa) at 0.1 MPa. The relationship between the rejection of the membrane with BSA 67 kDa, PEG 50 kDa, and PEG 20 kDa at different temperatures is
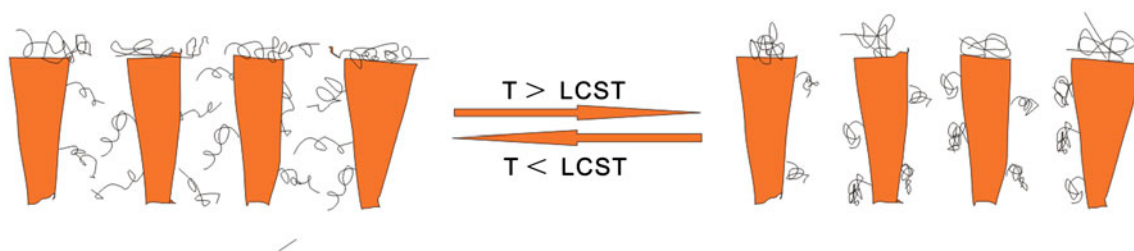
Fig. 10. The schematic of change of surface of temperature-sensitive membrane pores at different temperatures.

shown in Fig. 11. It shows that the rejection of M_3 with different molecular weight substances decreased as the temperature increased. It is clear that all the rejection of M_3 with different molecular weight substances depends little on the temperature; when the temperature is lower than 30℃. When the temperature is higher than 45℃, the rejection of M_3 decreases, while that of others decreased slightly. For example, The rejection of M_3 with BSA, PEG 50 (kDa) and PEG (20 kDa) were 95.4%, 91.5%, 64.6% at 40℃ decreased to 90.4%, 80.6%, 12.6% at 60℃, respectively. The capability of the blended membranes can be used for the proteins classification which will be next research work. In a word, the separation of different substances could be achieved by changing the temperature.

The effects of NIPAAm content in NPGs on rejection property of membranes were investigated with 1.0 g/L BSA and PEG (20 kDa) at 0.1 MPa. Take M_3 and M_4 for example, the relationship between the rejection of the membrane with different molecular weight substances is shown in Fig. 12.

Fig. 12 (a) shows that the rejection of membranes (M_3 and M_4) with PEG(20 kDa) decreased apparently compared with M_0 as the temperature increased. The

reduced value of M_3 was maximum. Additionally, the rejection of membranes (M_3 and M_4) remained constant over 90% at 10℃, which decreased to 12.6% and 66.7% at 60℃, respectively. While, the rejection of pure membrane M_0 was 99.6% at 10℃ and 85.3% at 60℃. The temperature-sensitive properties of membranes caused the rejection change.
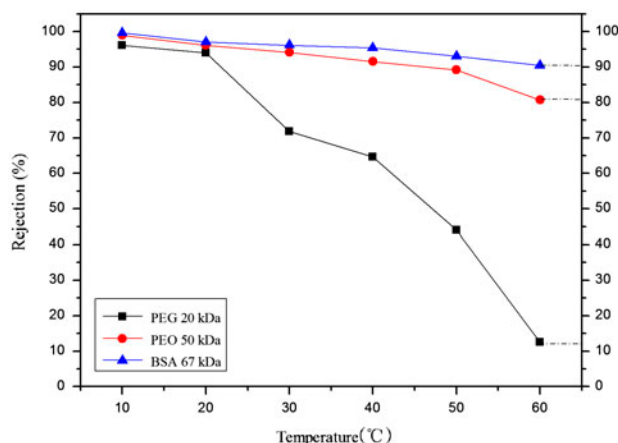

Fig. 11. Rejection of M_3 with different molecular weights (BSA 67 kDa, PEG 50 kDa, and PEG 20 kDa).
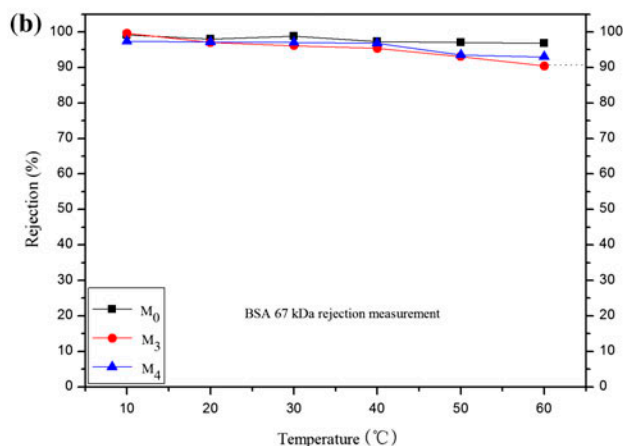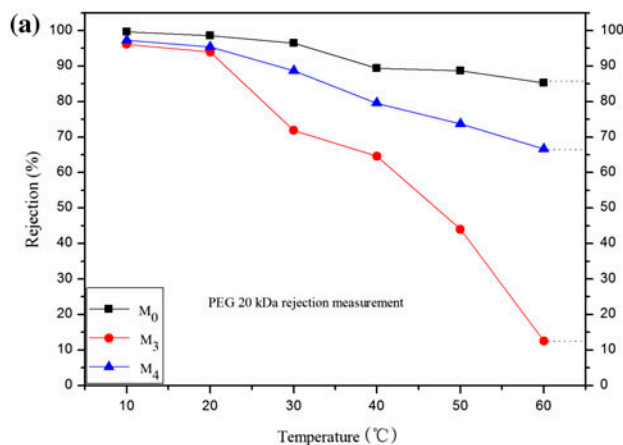
Fig. 12. Comparison of rejection of temperature-sensitive membranes (M_3 and M_4) with different molecular weights (a: PEG 20 kDa (12a) and b: BSA 67 kDa).

Fig. 12(b) shows that the rejection changed was not significant when the molecular weight was above 67 kDa for the membranes. For example, the rejection of M_3 with BSA was 97.0% at 20 ℃ which decreased to 90.4% at 60 ℃. The results show that the greater the molecular weight of the substances, the greater the rejection for the same membranes. For example, the rejection of M_3 with PEG (20 kDa) was 93.9% at 20 ℃ and 12.6% at 60 ℃, respectively. Therefore, the separation of different substances could be achieved by changing the temperature. It was because the changes of the pores with different temperatures lead to the change of rejection for different molecular weight substances.

4. Conclusions

Temperature-sensitive NPGs have been synthesized successfully from the two monomers NIPAAm and PEGMA by solution method. The obtained NPGs had different LCSTs by changing the mass ratios of the two monomers. All the copolymers exhibited higher LCSTs (44–53℃) than poly(N-isopropyl acrylamide) (near 32℃) in the water solution. The temperature-sensitive NPGs were added to the casting solutions, that preparer membranes with different temperature response performances. The addition of NPGs influenced the membrane properties and morphologies. The temperature-sensitivity of the modified membranes could be regulated by controlling the monomer PEGMA content in NPGs. The modified membranes had higher fluxes than pure PVDF membrane, while the membranes blended by NPG-0.6 and NPG-1.2 had 3.2 and 2.1 times higher fluxes than pure PVDF membrane at 55℃, respectively. Further reducing the monomer PEGMA content in NPGs, taking NPG-1.8 for example, the water fluxes of the membrane had 1.9 times higher flux than pure PVDF membrane at 55℃. Importantly, the NPGs had significant influences on the selectivity (for PEG and protein). The rejection of the same membrane with different molecular weight substances (BSA, PEG 20 kDa) at different temperatures explained that substance separation could be achieved by changing the temperatures. The decrease of contact angle showed that the modified membranes exhibited better hydrophilicity than pure PVDF membrane.

Acknowledgments

References

[1] P. Le-Clech, E.K. Lee, V. Chen, Hybrid photocatalysis/membrane treatment for surface waters containing low concentrations of natural organic matters, Water Res. 40 (2006) 323–330.

[2] M. de Souza Araki, C. de Morais Coutinho, L.A.G. Gonçalves, L.A. Viotto, Solvent permeability in commercial ultrafiltration polymeric membranes and evaluation of the structural and chemical stability towards hexane, Sep. Purif. Technol. 71 (2010) 13–21.

[3] P. Wang, M.M. Teoh, T.S. Chung, Morphological architecture of dual-layer hollow fiber for membrane distillation with higher desalination performance, Water Res. 45 (2011) 5489–5500.

[4] Y.K. Ong, N. Widjojo, T.S. Chung, Fundamentals of semi-crystalline poly(vinylidene fluoride) membrane formation and its prospects for biofuel (ethanol and acetone) separation via pervaporation, J. Membr. Sci. 378 (2011) 149–162.

[5] P. Sukitpaneenit, T.S. Chung, Molecular design of the morphology and pore size of PVDF hollow fiber membranes for ethanol–water separation employing the modified pore-flow concept, J. Membr. Sci. 374 (2011) 67–82.

[6] Z.-H. Zhao, L. Li, F.-W. Wu, S.-J. Tan, Z.-B. Zhang, The application of the modified PVDF ultrafiltration membranes in further purification of Ginkgo biloba extraction, J. Membr. Sci. 255 (2005) 125–131.

[7] E. Yuliwati, A.F. Ismail, Effect of additives concentration on the surface properties and performance of PVDF ultrafiltration membranes for refinery produced wastewater treatment, Desalination 273 (2011) 226–234.

[8] N.A. Ochoa, M. Masuelli, J. Marchese, Effect of hydrophilicity on fouling of an emulsified oil wastewater with PVDF/PMMA membranes, J. Membr. Sci. 226 (2003) 203–211.

[9] E. Yuliwati, A.F. Ismail, T. Matsuura, M.A. Kassim, M.S. Abdullah, Effect of modified PVDF hollow fiber submerged ultrafiltration membrane for refinery wastewater treatment, Desalination 283 (2011) 214–220.

[10] A. Hamza, V.A. Pham, T. Matsuura, J.P. Santerre, Development of membranes with low surface energy to reduce the fouling in ultrafiltration applications, J. Membr. Sci. 131 (1997) 217–227.

[11] Y.-H. Zhao, K.H. Wee, R.-B. Bai, A novel electrolyte-responsive membrane with tunable permeation selectivity for protein purification, ACS Appl. Mater. Intrer. 2 (2010) 203–211.

[12] D. Lee, A.J. Nolte, A.L. Kunz, M.F. Rubner, R.E. Cohen, pH-Induced hysteretic gating of track-etched polycarbonate membranes: Swelling/deswelling behavior of polyelectrolyte multilayers in confined geometry, J. Am. Chem. Soc. 128 (2006) 8521–8529.

[13] I. Tokarev, M. Orlov, S. Minko, Responsive polyelectrolyte gel membranes, Adv. Mater. 18 (2006) 2458–2460.

[14] M. Ulbricht, Advanced functional polymer membranes, Polymer 47 (2006) 2217–2262.

[15] E.S. Gil, S.M. Hudson, Stimuli-reponsive polymers and their bioconjugates, Prog. Polym. Sci. 29 (2004) 1173–1222.

[16] Y. Qiu, K. Park, Environment-sensitive hydrogels for drug delivery, Adv. Drug Deliv. Rev. 53 (2001) 321–339.

[17] S. Fujishige, K. Kubota, I. Ando, Phase transition of aqueous solutions of poly(N-isopropylacrylamide) and poly(N-isopropylmethacrylamide), J. Phys. Chem. 93 (1989) 3311–3313.

[18] K. Kubota, S. Fujishige, I. Ando, Single-chain transition of poly(N-isopropylacrylamide) in water, J. Phys. Chem. 94 (1990) 5154–5158.

[19] M. Marchetti, S. Prager, E.L. Cussler, Thermodynamic predictions of volume changes in temperature-sensitive gels. 1. Theory, Macromolecules. 23 (1990) 1760–1765.

[20] R. Xie, Y. Li, L.-Y. Chu, Preparation of thermo-responsive gating membranes with controllable response temperature, J. Membr. Sci. 289 (2007) 76–85.

[21] I. Tokarev, S. Minko, Stimuli-responsive porous hydrogels at interfaces for molecular filtration, separation, controlled release, and gating in capsules and membranes, Adv. Mater. 22 (2010) 3446–3462.

[22] H.-X. Guo, C.-L. Geng, Z.-P. Qin, C.-X. Chen, Hydrophilic modification of HDPE microfiltration membrane by corona-induced graft polymerization, Desalin. Water Treat. 51 (2013) 3810–3813.

[23] Y. Li, L.-Y. Chu, J.-H. Zhu, H.-D. Wang, S.-L. Xia, W.-M. Chen, Thermo-responsive gating characteristics of poly(N-isopropylacrylamide)-grafted porous polyvinylidene fluoride membranes, Ind. Eng. Chem. Res. 43 (2004) 2643–2649.

[24] M. Yang, L.-Y. Chu, Y. Li, X.-J. Zhao, H. Song, W.-M. Chen, Themo-responsive gating characteristics of Poly (N-isopropylacrylamide)-grafted membranes, Chem. Eng. Technol. 29 (2006) 631–636.

[25] P.S. Yune, J.E. Kilduff, G. Belfort, Fouling-resistant properties of a surface-modified poly(ether sulfone) ultrafiltration membrane grafted with poly(ethylene glycol)-amide binary monomers, J. Membr. Sci. 377 (2011) 159–166.

[26] Y.-J. Zhao, S.-Y. Zhou, M.-S. Li, A. Xue, Y. Zhang, J.-G. Wang, W.-H. Xing, Humic acid removal and easy-cleanability using temperature-responsive ZrO$_2$ tubular membranes grafted with poly(N-isopropylacrylamide) brush chains, Water Res. 47 (2013) 2375–2386.

[27] X. Feng, Y.-F. Guo, X. Chen, Y.-P. Zhao, J.-X. Li, Membrane formation process and mechanism of PVDF-g-PNIPAAm thermo-sensitive membrane, Desalination 290 (2012) 89–98.

[28] J.-Y. Wang, Y.-Y. Xu, L.-P. Zhu, J.-H. Li, B.-K. Zhu, Amphiphilic ABA copolymers used for surface modification of polysulfone membranes, Part 1: Molecular design, synthesis, and characterization, Polymer 49 (2008) 3256–3264.

[29] J.Z. Yu, L.P. Zhu, B.K. Zhu, Y.Y. Xu, Poly(N-isopropylacrylamide) grafted poly(vinylidene fluoride) copolymers for temperature-sensitive membranes, J. Membr. Sci. 366 (2011) 176–183.

[30] F. Liu, N.A. Hashim, Y. Liu, M.R. Abed, K. Li, Progress in the production and modification of PVDF membranes, J. Membr. Sci. 375 (2011) 1–27.

[31] C.-F. Di, X.-S. Jiang, J. Yin, Synthesis of stimuli-responsive star-Like copolymer H$_2$O- PNIPAm-r-PEG-

MA via the ATRP copolymerization technique and its micellization in aqueous solution, J. Appl. Polym. Sci. 115 (2010) 1831–1840.

[32] M.-H. Dan, Y. Su, X. Xiao, S.-T. Li, W.-Q. Zhang, A new family of thermo-responsive polymers based on poly [N-(4-vinylbenzyl)-N,N-dialkylamine], Macromolecules 46 (2013) 3137–3146.

[33] X.-L. Zhang, H.-L. WangQ.-Y. Gao, Preparation of temperature sensitive hydrogel poly(NIPAAm-PEG-MA) and its property, Mod. Chem. Indus. (China) 28 (2008) 54–56.

[34] R.H. Vora, P.S.G. Krishnan, S.H. Goh, T.S. Chung, Synthesis and properties of designed low-k fluoro-copoly ether imides, Adv. Funct. Mater. 11 (2001) 323–336.

[35] C.-W. Chen, M.-Q. Chen, T. Serizawa, M. Akashi, In-situ formation of silver nanopaticals on poly(N-isopropy lacrylamide)-coated polystyrene microspheres, Adv. Mater. 10 (1998) 1122–1126.

[36] X.-M. Ma, X.-Z. Tang, Preparation and properties of temperature-sensitive N-isopropyl acrylamid copolymer microgels containing functional hydroxyl groups in side chains, Acta plymerica sinica 8 (2006) 937–943.

[37] A.Y.C. Koh, R.K. Heenan, B.R. Saunders, A study of temperature-induced aggregation of responsive comb copolymers in aqueous solution, Phys. Chem. Chem. Phys. 5 (2003) 2417–2423.

[38] H.K. Ju, S.Y. Kim, Y.M. Lee, pH/temperature-responsive behaviors of semi-IPN and comb-type graft hydrogels composed of alginate and poly(N-isopropylacrylamide), Polymer 42 (2001) 6851–6857.

[39] H. Kawasaki, S. Sasaki, H. Maeda, Effect of introduced electric charge on the volume phase transition of N-isopropylacrylamide, J. Phys. Chem. B. 101 (1997) 4184–4187.

[40] H.-W. Chen, J.-F. Li, Y.-W. Ding, G.-Z. Zhang, Folding and unfolding of individual PNIPAM-g-PEO copolymer chains in dilute aqueous solutions, Macromolecules 38 (2005) 4403–4408.

[41] D. Singh, D. Kuckling, V. Choudhary, H. Adler, V. Koul, Synthesis and characterization of poly(N-isopropylacrylamide) films by photopolymerization, Polym. Adv. Technol. 17 (2006) 186–192.

[42] H.Y. Jung, J.K. Park, Blend membranes based on sulfonated poly(ether ether ketone) and poly(vinylidene fluoride) for high performance direct methanol fuel cell, Electrochim. Acta 52 (2007) 7464–7468.

[43] R.E. Kesting, Synthetic Polymeric Membranes: A Structural Perspective, John Wiley & Sons, New York, NY, 1985, pp. 85–237.

[44] N.A. Hashim, F. Liu, K. Li, A simplified method for preparation of hydrophilic PVDF membranes from an amphiphilic graft copolymer, J. Membr. Sci. 345 (2009) 134–141.

[45] B. Jung, Preparation of hydrophilic polyacrylonitrile blend membranes for ultrafiltration, J. Membr. Sci. 229 (2004) 129–136.

[46] N.A. Ochoa, M. Masuelli, J. Marchese, Effect of hydrophilicity on fouling of an emulsified oil wastewater with PVDF/PMMA membranes, J. Membr. Sci. 226 (2003) 203–211.

[47] J.-Q. Meng, C.-L. Chen, L.-P. Huang, Q.-Y. Du, Y.-F. Zhang, Surface modification of PVDF membrane via AGET ATRP directly from the membrane surface, Appl. Surf. Sci. 257 (2011) 6282–6290.